AD-A140 866 HIGH-TEMPERATURE OXIDATION OF ALPHA NICKEL-SILICON I 1/1
REACTION KINETICS - THERMOGRAVIMETRY(U) MATERIALS
RESEARCH LABS ASCOT VALE (AUSTRALIA) L D PALMER FEB 84
UNCLASSIFIED MRL-R-887 F/G 11/6 NL

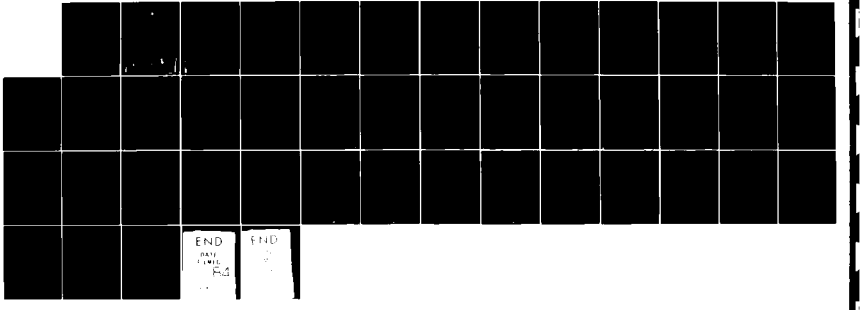

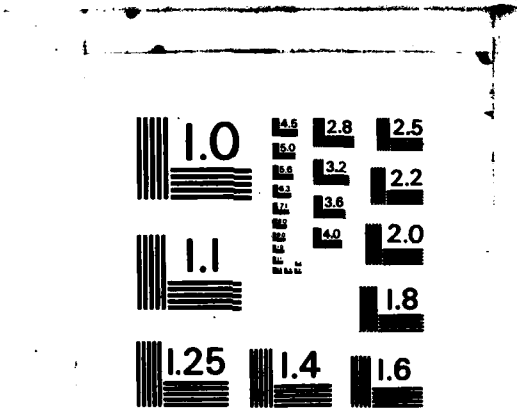

MICROCOPY RESOLUTION TEST CHART

NATIONAL BUREAU OF STANDARDS-1963-A

MRL-R-887

AR-003-300

DEPARTMENT OF DEFENCE

DEFENCE SCIENCE AND TECHNOLOGY ORGANISATION

MATERIALS RESEARCH LABORATORIES

MELBOURNE, VICTORIA

REPORT

MRL-R-887

HIGH-TEMPERATURE OXIDATION OF ALPHA NICKEL-SILICON: I. REACTION KINETICS - THERMOGRAVIMETRY

Lawrence D. Palmer*

* Dr Palmer was formerly of Metallurgy Division, Materials Research Laboratories, Maribyrnong, Victoria; he is now with the Ampol Research and Development Laboratory, Brisbane, Queensland.

DEPARTMENT OF DEFENCE

MATERIALS RESEARCH LABORATORIES

REPORT

MRL-R-887

HIGH-TEMPERATURE OXIDATION OF ALPHA NICKEL-SILICON: I. REACTION KINETICS - THERMOGRAVIMETRY

Lawrence D. Palmer

ABSTRACT

This report presents the results of a study of the reaction kinetics of the high-temperature oxidation of alpha binary nickel-silicon alloys and the thermocouple alloy Nisil. Rates of oxidation at temperatures in the range from 850 to 1250°C were measured by thermogravimetric methods under both isothermal and cyclic temperature conditions for periods of up to 164 h. Silicon in the alloys provides enhanced protection against high-temperature oxidation. Of the alloys studied, Nisil - a nickel-silicon-magnesium alloy - exhibited the greatest resistance to high-temperature oxidation. The agreement of the kinetic data with a simple parabolic rate law was assessed. For the low-silicon alloy Ni-0.9Si, the parabolic rate constant showed little variation throughout 164 h oxidation tests, whereas the rate constants for higher-silicon alloys generally decreased with time. This behaviour is discussed in terms of the diffusion of reactants through the growing oxide scales, whose composition and mechanical integrity may vary with time. An activation energy of 175 ± 21 kJ mol^{-1} was derived for the high-temperature oxidation of Ni-0.9Si.

POSTAL ADDRESS: Director, Materials Research Laboratories
P.O. Box 50, Ascot Vale, Victoria 3032, Australia

A1

SECURITY CLASSIFICATION OF THIS PAGE UNCLASSIFIED

DOCUMENT CONTROL DATA SHEET

REPORT NO.	AR NO.	REPORT SECURITY CLASSIFICATION
MRL-R-887	AR-003-300	UNCLASSIFIED

TITLE

HIGH-TEMPERATURE OXIDATION OF ALPHA NICKEL-SILICON:
I. REACTION KINETICS - THERMOGRAVIMETRY

AUTHOR(S)

LAWRENCE D. PALMER

CORPORATE AUTHOR
Materials Research Laboratories
P.O. Box 50,
Ascot Vale, Victoria 3032

REPORT DATE	TASK NO.	SPONSOR
FEBRUARY 1984	DST 82/129	

CLASSIFICATION/LIMITATION REVIEW DATE	CLASSIFICATION/RELEASE AUTHORITY
	Superintendent, MRL Metallurgy Division

SECONDARY DISTRIBUTION

Approved for Public Release

ANNOUNCEMENT

Announcement of this report is unlimited

KEYWORDS

Nickel alloys
Silicon containing alloys
Oxidation
Nickel silicon alloys
Nisil
High temperature oxidation
Reaction kinetics

COSATI GROUPS 1106

ABSTRACT

This report presents the results of a study of the reaction kinetics of the high-temperature oxidation of alpha binary nickel-silicon alloys and the thermocouple alloy Nisil. Rates of oxidation at temperatures in the range from 850 to 1250°C were measured by thermogravimetric methods under both isothermal and cyclic temperature conditions for periods of up to 164 h. Silicon in the alloys provides enhanced protection against high-temperature oxidation. Of the alloys studied, Nisil - a nickel-silicon-magnesium alloy - exhibited the greatest resistance to high-temperature oxidation. The agreement of the kinetic data with a simple parabolic rate law was assessed. For the low-silicon alloy Ni-0.9Si, the parabolic rate constant showed little variation throughout 164 h oxidation tests, whereas the rate constants for higher-silicon alloys generally decreased with time. This behaviour is discussed in terms of the diffusion of reactants through the growing oxide scales, whose composition and mechanical integrity may vary with time. An activation energy of 175 ± 21 kJ mol^{-1} was derived for the high-temperature oxidation of Ni-0.9Si.

SECURITY CLASSIFICATION OF THIS PAGE

UNCLASSIFIED

CONTENTS

HIGH-TEMPERATURE OXIDATION OF ALPHA NICKEL-SILICON:

I. REACTION KINETICS - THERMOGRAVIMETRY*

1. INTRODUCTION

A principal propulsion system for military weapons platforms is the gas turbine engine. Nickel- and cobalt-base superalloy components of the hot stages of such engines are required to maintain both the required mechanical properties and surface integrity for long periods of time at high temperatures in an extremely aggressive combustion environment. Attempts to improve mechanical properties by modifying chemical composition have generally produced alloys with lower resistance to high-temperature degradation by processes such as hot corrosion**.

In Australia, excessive oxidation and hot corrosion of gas turbine aerofoil components, which operate predominantly in the marine environment, have necessitated replacement of costly superalloy components after relatively short periods of service. Research at MRLM is aimed at finding ways and means of inhibiting processes of high-temperature degradation, so that gas turbine aerofoil components will show more stable properties and have longer lives. This research includes studies of the individual and synergistic influences of certain alloying elements on the high-temperature air oxidation characteristics both of the superalloys themselves and of the metallic

---

* This report is one of a series of seven complementary scientific papers (1-7) on research carried out in the High-Temperature Properties Group of Metallurgy Division, MRLM, on the high-temperature air oxidation of nickel and alpha nickel-silicon.

** Hot corrosion, in this context, is defined as the combined attack on the surface of gas turbine components by high-temperature exhaust gases from the combustor (which are highly oxidising and normally sulphur-bearing) and condensed phases (either liquid or solid) in particular salts.

coatings which are applied to protect them from degradation.

It is well known that the oxidation resistance of the base metals nickel, cobalt and iron at high temperatures can be substantially improved by alloying additions of aluminium and chromium, and also silicon. These elements increase resistance to oxidation by virtue of the properties of their oxides which, in general, are more effective barriers to the diffusion of reactant species, e.g. nickel and oxygen, (see Fig. 1), than the oxides of the base metal. The protective properties of such oxides have been exploited in the development of alloys to meet the demands of modern technology including those employed in the gas turbine engine. Although considerable progress has been made in formulating superalloys to satisfy the demanding requirements of the gas turbine, the contribution of individual alloying elements to the oxidation and hot-corrosion resistance of these multicomponent alloys is far from being well understood. This situation is exemplified by statements such as "the addition of silicon (to superalloys) has a marked effect in reducing the susceptibility to 'green-rot'* attack. The mechanism by which this works is not clear" (8).

In the past, in imparting high-temperature corrosion resistance to both the superalloys and their protective coatings, main reliance has been placed on the alloying elements chromium and aluminium. The full potential of silicon in this role seems not to have been realized, either in alloys or in coatings. The use of silicon in conventional superalloys has been limited to an extent, because of the deleterious effects which this element has upon mechanical properties (9). It is believed, however, that no such limitation exists in relation to the beneficial effects which silicon may have in enhancing the high-temperature corrosion resistance of metallic coatings, such as those which rely for protection on oxide layers of alumina or chromia over coating alloy structures based in NiAl or CoAl.

This report presents the results of a study of the reaction kinetics of the high-temperature oxidation of the alpha binary nickel-silicon (α-Ni-Si) alloys. Pure nickel is included in this study because it serves as a basis for comparison for the alloys. A complementary report (6) describes metallographic studies of the oxidized samples, in which the oxides responsible for improving oxidation resistance are characterized. The α-Ni-Si alloys themselves are of little technological significance, but studies such as this provide a necessary base for a better understanding of more complex systems such as the thermocouple alloy Nisil, Ni-4.4Si-0.1Mg** (10), which is also included, and high-temperature gas turbine materials.

Only a few studies of the kinetics of the high-temperature oxidation of α-Ni-Si alloys have been reported. Gil'dengorn and Rogel'berg (11) studied the oxidation in air of various alloys of 0.9 to 6.4 Si at 1000, 1100

---

* 'green-rot' is generally regarded as being a form of accelerated selective oxidation which occurs in partially oxidizing atmospheres.

** In this report alloy compositions are expressed as percentages by weight.

and 1200°C for periods of 10 and 50 h. Saegusa (12) reported studies in pure oxygen of various alloys of 0.5 to 3.2 Si. Isothermal experiments were carried out at 800, 1000 and 1200°C for 16 h periods, and alloys were also oxidized with the temperature increasing from 300 to 1300°C at a rate of 4°C min^{-1}. In another study, Kerr and Simkovich (13) oxidized various alloys with silicon concentrations up to 10.0 percent in pure oxygen at 1000°C for 33 h. In the present work, a number of different alpha alloys were heated for longer times, usually 164 h, and the accuracy of the weight and temperature data is substantially improved (1,2) compared with previous studies.

2. EXPERIMENTAL TECHNIQUES

The quantitative characteristics of the oxidation kinetics of the alloys under study were determined thermogravimetrically by continuously monitoring the weight of samples heated in air at temperatures in the range 850 to 1250°C. For α-Ni-Si alloys oxidized under these conditions, weight losses due to volatilization are negligible, and the measured weight gains can be considered to be due to oxygen uptake. Experiments were initiated by elevating the preheated furnace to surround samples suspended from a Cahn RH microbalance, thereby heating them to the experimental temperature within a few minutes. The thermogravimetric equipment, and the special techniques used to minimize uncertainties in the weight-gain and temperature data, are described elsewhere (1,2).

All thermogravimetric experiments were duplicated to assess the reproducibility of the weight gain curves. For cases where a duplicate experiment yielded a significantly different weight gain curve, an averaged curve is presented, and error bars are used to represent the deviation of the individual experiments (see for example Fig. 2).

Cylindrical samples of diameter 3 mm and length 35 mm were prepared from wire supplied by the manufacturer in the bright annealed condition, except for Ni-4.7Si which was supplied with a thin black oxide coating. Alloy compositions are given in Table 1. Since oxidation rates are often sensitive to the preparation of the specimen surface, a preparative procedure (3) designed to produce minimum surface damage and deformation was used. This procedure, which has the advantage of yielding oxidation rates for nickel whose repeatability is exceptionally high (3), involved the following sequential steps -

(i) **Grinding:** The outermost part (130 μm of radius) of the rod was removed by cylindrical grinding with a fine-grained silicon carbide wheel taking successive shallow cuts of 2.5 μm.

(ii) **Annealing:** The ground samples were annealed in argon (oxygen partial pressure <0.6 Pa) for 30 min at 800°C.

(iii) **Tumbling:** The samples were gently abraded in a slowly rotating suspension of 5 μm alumina powder in aviation-grade kerosene,

together with nickel balls. The tumbling removed approx. 0.1 μm of metal surface during a period of 100 h, including the thin oxide which formed during annealing.

(iv) Cleaning: The samples were cleaned ultrasonically in distilled water, ethanol and petroleum ether, and vapour degreased in petroleum ether and acetone.

3. OXIDATION KINETICS

3.1 Isothermal Oxidation

Oxidation kinetics for various alloys were determined at 1000, 1100 and 1200°C. Specific weight gains at 1100°C, the temperature at which the most comprehensive range of alloys was studied, are shown in Figs. 2, 3 and 4 for short-, medium-, and long-term exposures. The curves show that, apart from only a few exceptions which are discussed below, the higher the silicon concentration in the alpha alloys the greater the oxidation resistance. The degree of oxidation resistance so imparted is significant, particularly after extended periods of time at high temperatures. For example, after 160 h at 1100°C, Ni-5.2Si gained only eight per cent of the weight gained by pure nickel.

In the early stages of oxidation ($t < 1$ h), the alloys with lower silicon concentrations oxidized at slightly faster rates than did pure nickel (see Fig. 2); after extended periods of oxidation, however, all the alloys examined showed increased oxidation resistance (Fig. 4). The α-Ni-Si alloys thus can be considered in two groups of higher- and lower-silicon concentrations. The lower-silicon alloys, Ni-0.9Si and Ni-1.9Si, had oxidation rates at 1100°C which, for the first few hours, were very similar to the rate for nickel; alloys with silicon concentrations > 3.1 per cent, however, showed marked deviations from the nickel rate after 10 min.

A second and partial exception to the rule that increase in silicon concentration imparts greater oxidation resistance to α-Ni-Si is seen in Fig. 4. Although the rates for Ni-4.2Si and Ni-4.7Si were less than that for Ni-3.1Si during the early hours of oxidation, the opposite was true for the longer term of exposure.

The influence of temperature on the oxidation rates of a lower-silicon alloy, Ni-0.9Si, and a higher-silicon alloy, Ni-5.2Si, is shown graphically in Figs. 5 and 6, respectively. The square of the specific weight gain is plotted to allow easier assessment of conformity with a simple parabolic rate law (see 'Discussion'). The oxidation rate for Ni-0.9Si increased rapidly with increasing temperature, whereas the rate for Ni-5.2Si was virtually insensitive to temperature variation.

Over the long term, the oxidation rate of Nisil was less than that of any of the binary α-Ni-Si alloys.

3.2 Cylic Temperature Oxidation

The effects of temperature cycles on the oxidation rates of selected alloys was investigated. The results supplement the information on the influence of temperature on oxidation rates presented in Section 3.1, and also yield information on the effect of cyclic temperature-induced oxide spallation on the oxidation rates.

Fig. 7 shows the weight gains for the alloys Ni-0.9Si and Ni-5.2Si as their temperatures were cycled continuously in the range 850 to 1250°C at a precisely controlled rate in the range 1.00 to 1.12°C min^{-1}. Weight gains for Ni-5.2Si were over an order of magnitude less than the gains for Ni-0.9Si. For Ni-0.9Si the rates of oxidation, which are very nearly proportional to the slopes of curves in Fig. 7, increased rapidly with temperature. This result is consistent with Fig. 5. The rate of oxidation at particular temperatures decreased progressively with increases in the total number of temperature cycles, as the oxide thickened. When the change in oxide thickness during a complete cycle became small compared with the total oxide thickness (e.g. cycle 7 in Fig. 7), the weight gain curves became symmetrical, with the oxidation rate for particular temperatures being almost equal for both increasing and decreasing temperatures. This was not so for Ni-5.2Si, as can be seen from cycle 9 in Fig. 7. For this alloy, oxidation rates at particular temperatures were much larger during the heating half of the cylce than during the cooling half. In fact, negative oxidation rates, corresponding to a small net weight loss of approximately 0.02 mg cm^{-2}, were observed as the temperature decreased through the range 1200 to 1170°C (see Fig. 7). A duplicate experiment with Ni-5.2Si revealed the same effect but with a smaller magnitude. In contrast to the results shown in Fig. 7, the duplicate experiment also revealed weight losses of approx. 0.05 mg cm^{-2} as the temperature decreased from 1020 to 920°C. These weight losses appear to be real and not the result of gas forces in the furnace (1), as tests with inert alumina samples failed to yield similar weight changes when the temperature was cycled. It is possible that this weight loss is caused by the spallation during cooling of very small particles of oxide, too small to be detected individually by the microbalance.

The oxide scales on alloys with Si > 3.1 detached almost completely from the alloy as oxidized samples were cooled from high temperature to room temperature. On the other hand alloys with Si < 1.9 tended to retain their oxide scale during cooling to room temperature. Fig. 8 compares the oxidation of a Ni-5.2Si sample which was first oxidized for 164 h at 1000°C, and then reheated after the oxide scale had spalled during rapid cooling to room temperature. A lower oxidation rate was observed during the reheating.

Another example of the effect of temperature cycles on the oxidation of Ni-5.2Si is shown in Fig. 9. Here, the temperature has been lowered to 460±20°C and 330±20°C in two cycles after isothermal oxidation at 1000°C for 62 h. In contrast to the results depicted in Fig. 8, practically none of the oxide had spalled after these cycles, although the rapid oxidation observed as

the samples resumed a temperature of 1000°C indicated cracking or partial detachment of the scale. After several hours, the oxidation rate had slowed to a value similar to the rate prior to the temperature cycling. For Nisil, Fig. 10 shows that a cycle from 1100 to 720°C and back produced some damage to the scale, but no gross oxide spallation.

4. DISCUSSION

4.1 Derivation of the Thickness of Oxide and Consumed-Metal from Thermogravimetric Data

The measurement of the amount of oxide formed for particular alloys (as in Figs. 2 to 7) provides important data for assessing the suitability and lifetime of alloys for high-temperature applications. The thickness of the oxide film, the quantity of metal consumed in oxide formation and, most importantly, the remaining quantity of useful metal can easily be calculated (1) when a single external oxide phase is formed, e.g. nickel oxide NiO on nickel.

For Ni-Si alloys the oxide phases NiO, silica SiO_2 and nickel silicate Ni_2SiO_4 form externally on the alloys (6). In addition to these external oxides, the lower-silicon alloys e.g. Ni-0.9Si and Ni-1.9Si form internal precipitates of SiO_2 in the alloy matrix (6). Thermogravimetry determines the overall weight gain due to formation of all oxide products, both internal and external, so the exact calculation of oxide thickness, and the depth of metal affected by oxidation is not possible from weight gain curves such as those in Figs. 2 to 4. Good estimates can be made, however, of the thicknesses of the external oxides at any time by using the conversion factors in Table 2. These factors give the external oxide thickness per unit of specific weight gain, the thicknesses having been measured either from micrographs of polished oxide sections (6) or from precise measurement of detached oxide pieces. The conversion factors show a progressive increase with increase in silicon content of the alloy. It is instructive to compare the thickness values of Table 2 with theoretical values based on densities of oxides (14), which for NiO, SiO_2 and Ni_2SiO_4 are 7.0, 8.3 and 6.7 μm per mg cm^{-2} of oxygen. The lowering of the experimental value for nickel below 7.0 is due to the formation of intergranular oxide (10 to 15 per cent of total) in the substrate metal (6). The increase in the experimental values with increased silicon content in the alloy results from an increased fraction of SiO_2 in the oxide (6). A comparison of theoretical and Table 2 values of thickness suggests that (i) the solid state reaction product Ni_2SiO_4, which forms at least to some extent from the primary oxides NiO and SiO_2 (6), causes little contraction of the overall oxide thickness; and (ii) the oxides formed on the higher-silicon binary alloys ([Si] > 3.1) are somewhat porous, being thicker than predicted on the basis of theoretical densities and thermogravimetric data.

Relatively accurate estimations of the thickness of metal consumed by oxidation, and hence the remaining quantity of useful metal, can be made

from the thermogravimetric data for the alloys forming only external oxides. For pure nickel, the factor for metal comsumption as nickel is converted to nickel oxide is 4.1 μm of metal per mg cm^{-2} of weight gain (1). Pure silicon, on oxidation to silica, has a consumption factor of 3.8 μm per mg cm^{-2} of weight gain (1). If the atomic sizes of nickel and silicon in the alloys are assumed to be approximately equal to their respective elemental values, a consumption factor of 4.0 ± 0.1 μm of alloy per mg cm^{-2} of weight gain applies for alpha alloys with [Si] > 3.1.

For the alloys which form both internal and/or grain boundary oxides i.e., Ni-0Si, Ni-0.9Si and Ni-1.9Si, accurate estimates of the thickness of consumed metal cannot be made from thermogravimetric results, and metallurgical information is required to complement the weight gain data. Consideration of the significant effect of consumed metal must generally take into account the effect of the non-external oxide on the property of interest. For example, with the 3 mm diameter nickel rods exposed at high temperatures in this study, about 20 per cent of the total original quantity of metal was oxidized, and most of the oxide was external. However, the 10 to 15 per cent of the intergranular oxide which formed throughout the metal reduced the mechanical strength of the remaining metal to such a low value that the whole rod could be considered to have been effectively consumed. The effect of internal oxides in Ni-0.9Si and Ni-1.9Si, by contrast with the intergranular oxides in nickel, is limited to depths only of the order of the thickness of the external oxides (6). Moreover, such internal oxide dispersions of SiO_2 could even have a strengthening effect on the alloy.

4.2 Agreement of the Thermogravimetric Data with Simple Rate Laws

For metals which form compact, adherent, relatively thick oxide films (>0.6 μm (15), the thickness regime of the present study), the thermogravimetric data are expected to agree, at least approximately, with a parabolic rate law, for which the oxidation rate is given by

$$\frac{d(\Delta W/A)}{dt} = \frac{k_p}{2} \frac{1}{(\Delta W/A)} \qquad (1)$$

where ΔW/A, the weight gain due to oxide formation per unit of surface area A, is linearly related to oxide thickness, and t is time. The parabolic rate constant, k_p, is expressed usually in units of (g of O)^2 cm^{-4} s^{-1}. If k_p is independent of time, eqn. (1) can be integrated to give the more familiar form of the parabolic rate law

$$(\Delta W/A)^2 = k_p t \qquad (2)$$

Eqns. (1) and (2) can be obtained simply from the intuitive assumption that, as the oxide scale thickens, the oxidation rate decreases according to eqn. (1). A more fundamental derivation of the parabolic rate law, which leads to a better understanding of the basic processes of high temperature oxidation, has been provided by Wagner (16). His model assumes that either the diffusion of reactant ions or the transport of electrons

through the growing oxide scale (see Fig. 1) is the step which determines the rate of oxide growth. In other words, the reaction steps which occur at metal/oxide and oxide/gas interfaces are rapid compared with the diffusion of reactants, e.g. nickel and oxygen, through the scale. These rapid interfacial reaction steps include the adsorption and dissociation of diatomic oxygen and the creation of metal ion vacancies, all of which occur at the oxide/gas interface, and consumption of metal ion vacancies at the metal/oxide interface.

The rate of oxide growth therefore depends primarily on the properties of the oxide scale, in particular its defect structure and electrical conductivity. NiO is a p-type electronic semiconductor, and it is the diffusion of reactant ions through the scale, and not the accompanying electronic transport, which governs the oxidation rate. The parabolic rate constant is given by eqn. (3) as

$$k_p = (\rho_{NiO}\, M_O/M_{NiO})^2 \int_{p_{O_2}^i}^{p_{O_2}^o} (\frac{m}{r} D_{Ni} + D_O)\, d\ln p_{O_2} \qquad (3)$$

for which ρ_{NiO} is the density of NiO,

M_O is the atomic weight of oxygen,

M_{NiO} is the molecular weight of NiO,

$p_{O_2}^i$ and $p_{O_2}^o$ are the oxygen pressures at the metal/oxide and oxide/gas interfaces, respectively, (see Fig. 1),

D_{Ni} and D_O are the lattice diffusion coefficients of nickel and oxygen in the oxide, and

m and r are the ionic charge for nickel and oxygen, respectively.

Eqn. (3) can be simplified by noting that

(i) $D_{Ni} >> D_O$ at oxygen pressures of the order of $p_{O_2}^o$ (17),

(ii) although D_{Ni} decreases and D_O is expected to increase as p_{O_2} decreases to $p_{O_2}^i$ (18), D_O will not make a significant contribution to the integral in eqn. (3) because oxygen defects are minority defects over the whole stability range of NiO (18),

(iii) m/r for NiO is unity, and

(iv) the diffusion coefficient D_{Ni} has a dependence on p_{O_2} (16) given by eqn. (4)

$$D_{Ni} = D^{r}_{Ni} \; p_{O_2}^{1/n} \tag{4}$$

where D^{r}_{Ni} is the diffusion coefficient at the convenient reference pressure 1.0 atm of oxygen. For singly charged vacancies n has the value 4 and for doubly charged vacancies it is 6; these are the two species generally considered to predominate at temperatures around 1100°C (19).
Eqn. (3) then reduces to

$$k_p = n \; (\rho_{NiO} \; M_O/M_{NiO})^2 \; (p^{o}_{O_2})^{1/n} \; D^{r}_{Ni} \tag{5a}$$

For oxidation in air at 1.0 atm, $p^{o}_{O_2} = 0.21$ atm and eqn. 5(a) becomes

$$\text{for singly charged vacancies } k_p = 5.5 \; D^{r}_{Ni} \tag{5b}$$

$$\text{and for doubly charge vacancies } k_p = 9.4 \; D^{r}_{Ni} \tag{5c}$$

with k_p having units of $g^2 \; cm^{-4} \; s^{-1}$ when D^{r}_{Ni} has units of $cm^2 \; s^{-1}$.

Parabolic rate constants for the oxidation of Ni at 1100°C, calculated from eqns. (5b) and (5c) and literature values for the diffusion coefficient D^{r}_{Ni}, are included in Table 3. The values differ by more than an order of magnitude, probably due to the sensitivity of the defect structure and doping effects in NiO to even relatively low concentrations of impurities (29). Parabolic rate constants derived directly from oxidation experiments, including those from this study, are also listed in Table 3, and they too differ considerably. It can be seen, however, that the range of the k_p values calculated from diffusion coefficients coincides reasonably well with the range of experimentally derived values. It can be argued, therefore, that the Wagner model provides a useful basis for understanding the high-temperature oxidation of nickel and its dilute alloys, and focusses attention on the importance of diffusion of nickel through the growing oxide scale. It should be remembered, however, that the oxidation of nickel is quite complex, with the rate depending strongly on purity, surface preparation (3) and specimen geometry (29,30). Furthermore, while outward diffusion of nickel ions through the NiO scale is the dominant lattice diffusion process, inward diffusion of oxygen via oxide grain boundaries also contributes to the oxidation rate (31).

The Wagner model predicts values of k_p for nickel which agree only approximately with the observed values. Moreover, the greater complexity of

the oxidation of α-Ni-Si alloys, with scales composed of NiO, SiO_2 and Ni_2SiO_4 (6), precludes a simple, basic quantitative description analogous to the Wagner model for nickel. Nevertheless, the defect structure and diffusion properties of the oxides provide a good qualitative understanding of the observed oxidation kinetics.

In the oxidation of silicon, at temperatures in the range 900 to 1200°C, oxygen diffuses through SiO_2 much faster than does silicon, but the oxygen diffusion coefficient is at least three orders of magnitude smaller (22) than the nickel diffusion coefficients presented in Table 2. Since the diffusion rate of nickel through SiO_2 would likewise be expected to be several orders of magnitude less (32) than the diffusion rate of nickel through nickel oxide, any SiO_2 in the oxide scale will be an effective barrier to the diffusion of the reactants nickel, silicon and oxygen. The oxidation rate for Ni-Si alloys will therefore be reduced significantly when silica is incorporated in the oxide scale. This reduction in oxidation rate will be greater for higher volume fractions of SiO_2, and for film-like SiO_2 morphology which will have optimum effect as a barrier to diffusion across the scale.

The spinel nickel silicate Ni_2SiO_4 has been identified in the scale on α-Ni-Si (6). It is likely that, after long periods at high temperatures, much of the SiO_2 originally present in the scale will have reacted with NiO to form Ni_2SiO_4. Little is known about the details of the diffusion mechanisms for these oxides, but from structural considerations it appears that the diffusion paths are complex (33). Various spinel oxides exhibit low diffusion rates (33), and from Fig. 4 it seems likely that Ni_2SiO_4 is no exception.

The measure of agreement of the experimental data for the oxidation of α-Ni-Si alloys with a general parabolic rate law can be assessed in two ways. In the first method, the instantaneous value of k_p is calculated using eqn. (1). The oxidation is assumed to be basically diffusion controlled, but it is recognized that k_p may vary with time due to changes in the diffusion characteristics of the scale. Such changes can readily occur in long-term alloy oxidation, as changes in the scale composition and morphology are likely to occur as the oxidation proceeds.

Values of k_p as a function of time for oxidation in air at 1100°C are presented in Figs. 11(a) and 11(b). The rates of oxidation $d(\Delta W/A)/dt$, or alternatively $d(\Delta W/A)^2/dt$, required for evaluating k_p from eqn. (1), were calculated using eqn. (6), namely (34),

$$\left[\frac{dy}{dt}\right]_{t_0,y_0} = \frac{-2y_{-2} - y_{-1} + y_1 + 2y_{-2}}{10\Delta t} \qquad (6)$$

This equation is based on a least-squares minimization and gives the slope of a function y(t) at (t_0,y_0) in terms of neighbouring points (t_{-2},y_{-2}), (t_{-1},y_{-1}), (t_1,y_1) and (t_2,y_2) which are separated from (t_0,y_0) by $-2\Delta t$, $-\Delta t$, Δt and $2\Delta t$, respectively. The alloy Ni-0.9Si oxidizes at 1100°C with a remarkably constant value for k_p for times from 0.1 to 160 h. Nickel

gives a similar constant value to 20 h, but the value increases between 20 and 160 h. The occurrence of this increase, following a relatively long period of constant k_p, suggests that for nickel a new factor, in addition to the usual diffusion processes, becomes significant. Mechanical failure of the thick oxide scale due to stresses occurring during oxidation (3,31) provides a possible explanation for this behaviour. If this is so, the silicon in the alloy Ni-0.9Si has very little apparent effect on the diffusion properties of the oxide scale formed during oxidation, since k_p for Ni-0.9Si is nearly equal to the early value for nickel.

The alloys with Si contents of 1.9 per cent or higher all give k_p values which decrease with time in the initial stages of oxidation (see Figs. 11(a) and 11(b)). In some cases, however, e.g. Ni-4.2Si and Ni-5.2Si, detectable increases in k_p occur as the scales thicken, again due possibly to the influence of oxidation stresses on the scales. The decrease in k_p with time for these alloys is most probably a consequence of an increase in the volume fraction of SiO_2 in the scale during oxidation. This mechanism can readily be appreciated for Ni-1.9Si, in which silicon is oxidized to SiO_2 internally; the surrounding nickel substrate is subsequently oxidized to form an inner layer of the external scale (6) as the reaction front at the alloy/scale interface recedes. For the externally oxidizing alloys (4.2, 4.7 and 5.2Si) also, progressive SiO_2 enrichment of the scale will occur. This is because silicon depletion of the unoxidised alloy substrate extends to significant depths after 164 h at 1100°C (6), and silicon oxidizes preferentially to nickel at the metal/oxide interface due to its greater negative free energy of formation (29). In the initial stages of oxidation, when the oxidation is the most rapid and the supply of oxygen to the metal is relatively unhindered by oxide diffusion-barriers, the silicon-to-nickel cation concentration ratio in the scale is expected to approximate that of the alloy prior to oxidation. This stage of the oxidation rapidly gives way to the oxide-diffusion controlled stage. During this stage the oxidation rate steadily decreases with time, and the diffusion of silicon outward through the alloy to the metal/oxide interface, and its preferential oxidation there, results in a continuous increase in the fraction of SiO_2 (or Ni_2SiO_4) in the scale, and hence a decrease in k_p.

In the second method of assessing the measure of agreement of the oxidation data with the parabolic rate law, a general rate law of the form

$$(\Delta W/A)^n = k\,t \qquad (7)$$

is assumed to apply with k in this case being independent of time. The value of the exponent n is obtained from the slope of a plot of log (ΔW/A) versus log t. The data for oxidation at 1100°C have been treated by this method in Fig. 12, and values of n are given in Table 4(a). Values of n for a lower-silicon alloy Ni-0.9Si and a higher-silicon alloy Ni-5.2Si at 1000, 1100 and 1200°C are shown in Table 4(b). Ni-0.9Si gives values of n close to the parabolic value of 2.0 for the three temperatures; Ni also gives values of n close to 2.0 at 1100°C, but only for the time range 0.1 to 20 h. The other alloys in most cases have values of n greater than 2.0, particularly during

the first few hours of oxidation, thus their rates of oxidation decrease with time more rapidly than would be expected from parabolic kinetics. Nisil, the most oxidation resistant of the alloys studied, gives very high values of m during the first hours of oxidation at 1100°C. Apparently, a thin but highly protective oxide film forms in the first few minutes of exposure at high temperature, and the high value of m during the first hour suggests that the protective nature of the scale continues to be enhanced during this period. Such a conclusion needs further careful consideration, however, because of the magnitude of experimental uncertainties inherent in the measurement of these very low rates of oxidation (see error bars on Fig. 12).

4.3 Influence of Temperature on Oxidation

Experimental results showing the influence of temperature on the oxidation of a lower-silicon alloy (Ni-0.9Si) and of a higher-silicon alloy (Ni-5.2Si) are presented in Figs. 5 to 7. The Wagner model and its application to the high-temperature oxidation of nickel at 1100°C was discussed in the previous section, and it also serves here as a useful basis for understanding how temperature influences the oxidation of nickel and α-Ni-Si alloys. For nickel, eqns. (5b) and (5c) show that the parabolic rate constant k_p is simply related to the diffusion coefficient of nickel ions in NiO. Since the diffusion coefficient has an Arrhenius dependence on temperature, given by

$$D = D_o \exp(-Q/R\,T) \qquad (8)$$

where Q is the activation energy, k_p will have nearly the same temperature dependence, since the temperature variations of the other terms in eqn. 5(a) are comparatively small. It should be remembered, however, that the nature of the diffusion processes controlling the oxidation are likely to change with temperature. At intermediate temperatures, defined by Lawless as 200 to 800°C (15), grain boundary diffusion will generally be more important than lattice diffusion. At high temperatures i.e. above about 1000°C for Ni, the activation energy Q for grain boundary diffusion is generally much less than that for lattice diffusion (16), making lattice diffusion the dominant diffusion process. Even in the high-temperature range, the mechanism of lattice diffusion can vary with temperature. For example, Fueki and Wagner (24) infer from their studies of the oxygen pressure dependence of the oxidation of nickel that, at 1300 and 1400°C, diffusion occurs via singly charged vacancies (eqn. (5b)) while, and at 1000 and 1100°C, it occurs via doubly charged vacancies (eqn. (5c)). For the α-Ni-Si alloys, the temperature dependence will also be influenced by the additional complexity that the composition and morphology of the scale will depend on the entire temperature history of the sample.

As noted previously, the silicon content of the alloy Ni-0.9Si appears to have had very little effect, at 1100°C, on the diffusion of reactants through the oxide scale. For this alloy, the temperature dependence of the oxidation process can probably be characterised in terms of a single

activation energy Q, with any variation in oxide scale composition with variation in temperature having little influence. An Arrhenius plot of the data from Fig. 5 is shown in Fig. 13, from which Q can be obtained from the slope.

Kofstad (35) gives another method of experimentally deriving activation energies; it involves heating alloys at precise rates of temperature variation, such as were used to obtain Figs. 7 and 8. The method combines eqns. (1), (5) and (8) to yield, for the case of parabolic kinetics,

$$\ln (\Delta W/A) + \ln d(\Delta W/A)/dt = \ln B - Q/R\,T \qquad (9)$$

where the constant B is relatively independent of temperature. A plot of the left-hand side of eqn. (9), as a function of reciprocal temperature for the alloy Ni-0.9Si, is presented in Fig. 13, from which Q can be derived from the slope. Fig. 13 shows the data for the two complete cycles of temperature 850 to 1250 to 850°C. Apart from the lower temperature regime, where experimental uncertainties are greatest due to low values of the oxidation rate and where lattice diffusion is probably less important than grain boundary diffusion, the data can be well fitted to a straight line to yield the activation energy Q. Weight gain data from duplicate experiments each consisting of 13 complete temperature cycles (see Fig. 7) were treated in this way. The average activation energies in the range 950 to 1250°C for each half-cycle of temperature are plotted in Fig. 14, together with the least-squares correlation coefficient γ, as a function of the temperature half-cycle number. For one of the duplicate experiments, Q values obtained during the cooling half-cycle were substantially higher than those from the heating half-cycle. As these high values had associated correlation coefficients $\gamma < 0.98$, they were considered to be less reliable than the other values. Averaging the 39 values of Q for which $\gamma > 0.98$ yields, for Ni-0.9Si at temperatures from 950 to 1250°C,

$$Q = 175 \pm 21 \text{ kJ mol}^{-1}$$

This value can be compared with the values derived from isothermal experiments (see Fig. 5). Calculation of Q using eqns. 2 and 8, and Fig. 5, yields an activation energy of 168 kJ mol^{-1} for temperatures from 1100 to 1200°C, and an activation energy of 220 to 250 kJ mol^{-1} from 1000 to 1100°C. Thus there is good agreement over the range 1100 to 1200°C. A determination of the activation energy from Kofstad's varying-temperature technique (35) is considered to be the more reliable, for two reasons. First, it effectively assesses Q at all temperatures in the range of interest, whereas Fig. 5 contains data for only three temperatures. Secondly, the varying-temperature method utilizes the same alloy samples over the whole temperature range. The advantage of this can readily be assessed from the scatter of k_p values from duplicate experiments in Fig. 5 and the large uncertainty so introduced to Q. Notwithstanding, the isothermal and varying-temperature techniques should be regarded as complementary. Isothermal experiments are necessary to establish

whether the kinetics are, in fact, parabolic over the temperature range of interest. Furthermore, as discussed previously, evaluation of activation energies is probably only profitable when the diffusion properties of the scale depend mainly on a single component. This appears to hold for the alloy Ni-0.9Si, because the experimentally derived activation energy agrees well with literature values for the oxidation of pure nickel, which have been summarized by Tomlison (28). The values range from 142 to 286 kJ mol^{-1}, with recent values of 226, 192, 180 and 159 kJ mol^{-1}, and Tomlinson's 174.4 ± 13.6 kJ mol^{-1}.

Treatment of the data in Fig. 7 for the higher-silicon alloy Ni-5.2Si by the method of Kofstad (35) failed to yield a constant value of the activation energy. This is not unexpected, since the composition of the scale will vary with both temperature and time. The time dependence of the fraction of SiO_2 in the scale has been discussed previously, and Fig. 6 provides evidence that, for isothermal oxidation, the scale composition does indeed vary with temperature. For the temperatures 1000, 1100 and 1200°C, there is virtually no increase in k_p, whereas an increase by a factor of 9.4 is expected on the basis of the activation energy for the oxidation of Ni-0.9Si; by a factor of 7.3 based on the activation energy for nickel diffusion through amorphous SiO_2 (32); and by 4.6 or 2.4 based on the activation energy for the oxidation of silicon in dry or wet oxygen, respectively (22). Apart from the possibility of formation of a different allotropic form of SiO_2 at the higher temperatures, the relative independence of k_p with respect to temperature therefore indicates that the fraction of SiO_2 in the scale increases with temperature.

Fig. 7 shows that, under conditions of varying temperature, the oxidation rate for the higher-silicon alloy Ni-5.2Si has complex dependences on both time and temperature. During the first cycle of heating from 850 to 1250°C the rate of oxidation, which is adequately measured by the slopes in Fig. 7, increases rapidly as the temperature rises from 1000 to 1100°C. This behaviour can be contrasted with the data in Fig. 6, for which the oxidation rate constants are relatively independent of temperature. During the period when the oxidation rate is increasing, the protective qualities of the scale are obviously being enhanced, since very low oxidation rates are observed for similar temperatures during the subsequent cooling part of the cycle. During cooling, the scale appears to suffer some mechanical damage, due presumably to mismatch of the coefficients of expansion of the oxide and the alloy. This is shown by the oxidation rate for a particular temperature being faster during the next heating cycle than it was during cooling. No gross spalling of the oxide occurs for temperature cycling between 850 and 1250°C.

5. ACKNOWLEDGEMENTS

The author wishes to thank Dr N.A. Burley, Head, High-Temperature Properties Group, Metallurgy Division MRL, for his helpful advice both during the research work and in the preparation of this paper.

Other members of High-Temperature Properties Group also contributed to this work. The author wishes to thank in particular Mr J. Saulitis, for provision of computer programs to process the large quantity of experimental data; also Mr S.D. Boyd, Mrs J.L. Cocking, Mr J.A. Coleman and Mr P.H. Price for assistance with the thermogravimetric experiments.

6. REFERENCES

1. Palmer, L.D. (1978) "A thermogravimetric system for investigating gas-metal reactions at elevated temperatures." *MRL Report 726.*

2. Palmer, L.D. (1980). "Sources of error in thermogravimetry : Balance inclination and specimen temperature." *J. Phys. E: Sci. Instrum.*, 13, 919-923.

3. Palmer, L.D. and Cocking, J.L. (1979). "Influence of surface preparation on the high-temperature oxidation of nickel." In *Microstructural Science*, Volume 7, (eds. I. Le May, P.A. Fallon and J.L. McCall) Elsevier North Holland, Inc.) pp. 193-202.

4. Palmer, L.D. (1982). "High-temperature oxidation of alpha nickel-silicon: I Reaction kinetics - thermogravimetry." *MRL Report* (this ;aper).

5. Burley, N.A. and Hess, R.M. "High-temperature oxidation of alpha nickel-silicon: II Reaction kinetics - thermoelectromotive force measurements." *MRL Report*, in course of publication.

6. Cocking, J.L. (1982). "High-temperature oxidation of alpha nickel-silicon: III Microstructures and mechanisms." *MRL Report*, in course of publication.

7. Cocking, J.L., Palmer, L.D., Burley, N.A. and Johnston, G.R. "High-temperature oxidation of alpha nickel-silicon." *Oxid. Met.*, in course of publication.

8. Eggar, J.W. (1974). *The Nimonic Alloys* (eds. W. Batteridge and J. Heslop), Edward Arnold, London, pp. 352-356.

9. Payne, B.E. ibid 8, p. 374.

10. Burley, N.A., Powell, R.L., Burns, G.W. and Scroger, M.G. (1978), "The nicrosil versus nisil thermocouple: Properties and thermoelectric reference data." *NBS Monograph 161*, US Govt. Printing Office, Washington.

11. Gil'dengorn, I.S. and Rogel'berg, I.L. (1965). 'High-temperature oxidation of nickel-silicon alloys." *Phys. Met. Metallog.* 17, 45-53.

12. Saegusa, F. (1969). 'Thermal Oxidation of Nickel-Silicon Alloys." In *Thermal Analysis*, Vol. 2, (eds. R.F. Schwenker and P.D. Garn), Academic Press, New York, pp. 893-907.

13. Kerr, T.W. and Simkovich, G. (1976). "Hot corrosion studies on nickel-based alloys containing silicon." In *Properties of High Temperature Alloys*, (eds. Z.A. Foroulis and F.S. Pettit), The Electrochemical Society, Princeton, pp. 576-584.

14. Weast, R.C. (1975). "Physical constants of inorganic compounds." and "X-ray crystallographic data of minerals." *Handbook of Chemistry and Physics*, 56th edition, CRC Press, Cleveland, pp. B-67 to B-234.

15. Lawless, K.R. (1974). "The oxidation of metals." *Rep. Prog. Phys.*, 37, 231-316.

16. Kofstad, P. (1966). *High Temperature Oxidation of Metals*, J. Wiley and Sons, New York, pp. 112-146.

17. O'Keefe, M. and Moore, W.J. (1961). "Diffusion of oxygen in single crystals of nickel oxide." *J. Phys. Chem.*, 65, 1438-9.

18. Kofstad, P. (1972). *Nonstoichiometry, Diffusion and Electrical Conductivity in Binary Metal Oxides*, Wiley-Interscience, New York, pp. 22-46.

19. Koel, G.J. and Gellings, P.J. (1972). "The contribution of different types of point defects on diffusion in CoO and NiO during oxidation of metals." *Oxid. Metals*, 5, 185-203.

20. Volpe, M.L. and Reddy, J. (1970). "Cation self-diffusion and semi-conductivity in NiO." *J. Chem. Phys.*, 53, 1117-1125.

21. Atkinson, A. and Taylor, R.I. (1978). "The self-diffusion of Ni in NiO and its relevance to the oxidation of Ni." *J. Mater. Sci.* 13, 427-432.

22. Kofstad, P. ibid 18, pp. 246-264 and pp. 349-355.

23. Phillips, W.L. (1963). "Oxidation rates of pure and less pure nickel." *J. Electrochem. Soc.*, 110, 1014-1015.

24. Fueki, K. and Wagner, J.B. (1965). "Studies of the oxidation of nickel in the temperature range of 900 to 1400°C." *J. Electrochem. Soc.*, 112, 384-388.

25. Sartell, J.A. and Li, C.H. (1961). "The mechanism of oxidation of high-purity nickel in the range 950-1250°C." *J. Inst. Metals*, 90, 92-96.

26. Berry, L. and Paidassi, J. (1962). "The oxidation kinetics of nickel in air at high temperatures." *C.R. Acad. Sci. Paris*, 255, 2253-5.

27. Caplan, D., Graham, M.J. and Cohen, M. (1972). "Effect on cold work on the oxidation of nickel at high temperature." *J. Electrochem. Soc.*, 119, 1205-1215.

28. Tomlinson, W.J. (1977). "Diffusion enthalpies and entropies in thermallyforming NiO and (Ni,Fe)O from 800-1200°C." *J. Chem. Soc., Faraday Trans.* 1, 73, 1334-9.

29. Wasielewski, G.E. and Rapp, R.A. (1972). "High-temperature oxidation." *In The Superalloys* (eds. C.T. Sims and W.C. Hagel), John Wiley & Sons, New York, pp. 287-316.

30. Hales, R. and Hill, A.C. (1972). "The role of metal lattice vacancies in the high temperature oxidation of nickel." *Corros. Sci.*, 12, 843-853.

31. Rhines, F.N. and Connell, R.G. (1975). "Influence of stress on the high temperature oxidation of nickel." In *Stress Effects and the Oxidation of Metals* (ed. J.V. Cathcart), Met. Soc. AIME, New York, pp. 94-113.

32. Ghoshtagore, R.N. (1969). "Diffusion of nickel in amorphous silicon dioxide and silicon nitride films." *J. Appl. Phys.*, 40, 4374-4376.

33. Kofstad, P. ibid 16, pp. 306-308.

34. Lanczos, C. (1957). *Applied Analysis*, Pitman and Sons, London, pp. 321-324.

35. Kofstad, P. (1957). "Oxidation of metals: Determination of activation energies." *Nature*, 179, 1362-1363.

TABLE 1

COMPOSITION OF ALLOYS (WEIGHT PER CENT)

Alloy	Analyst	Si	Mg	Fe	Al	Co	Zr	Mn	C	Cu	Ti	Ni
Nickel-270	Manuf.[a]	<.005	<.005	<.02	<.005			<.005	<.02	<.005	<.005	99.97
	MRL	<.0005	nd[a]	.012	<.0001			vft[a]	.022	<.001	nd	bal[a]
Ni-0.9Si	Manuf.	.088	.004			.05	.026		.006			bal
	MRL	0.86	vft	.02		.04	.03	nd	.018			bal
Ni-1.9Si	Manuf.	1.88	.004			.04	.033		.009			bal
	MRL	1.85	ft[a]	.03		.04	.01	nd	.006			bal
Ni-3.1Si	Manuf.	3.08	.004			.05	.038		.009			bal
	MRL	3.11	ft	.03		.04	.01	nd	.006			bal
Ni-4.2Si	Manuf.	4.12	.004			.04	.024		.011			bal
	MRL	4.16	ft	.04		.04	.02	nd	.006			bal
Ni-4.7Si	Manuf.	4.69	.004	.06		.008	.03		.02	.002	.002	bal
	MRL	4.65	.003	.05					.021			bal
Ni-5.2Si	Manuf.	5.09	.004			.05	.036		.006			bal
	MRL	5.18	ft	.04		.04	.01	nd	.002			bal
Nisil	Manuf.	4.25	.11	.03				.02	.011			bal
	MRL	4.36	.11	.04				.01	.006			bal

[a]Manuf. = manufacturer; nd = not detected; ft = faint trace; vft = very faint trace; bal = balance

TABLE 2

THICKNESS OF EXTERNAL OXIDE PER UNIT OF WEIGHT GAIN

Alloy	Thickness/specific weight gain, μm/(mg of oxygen cm^{-2})
Nickel-270	6.1 ± 0.3
Ni-0.9Si	7.1 ± 0.4
Ni-1.9Si	7.5 ± 0.6
Ni-3.1Si	8.9 ± 1.0
Ni-4.2Si	8.7 ± 0.7
Ni-4.7Si	10.3 ± 0.7
Ni-5.2Si	10.6 ± 1.2
Nisil	6.3 ± 1.3

TABLE 3

COMPARISON OF k_p VALUES DERIVED FROM DIFFUSION COEFFICIENTS AND FROM OXIDATION EXPERIMENTS AT 1100°C IN AIR

D^r_{Ni} (a,g) $cm^2\ s^{-1}$	Ref.	k_p [from eqn. (5b)] $g^2\ cm^{-4}\ s^{-1}$	k_p [from eqn. (5c)] $g^2\ cm^{-4}\ s^{-1}$	k_p [from oxidation] $g^2\ cm^{-4}\ s^{-1}$	Ref.
1.0×10^{-11}	(20)	0.55×10^{-10}	0.94×10^{-10}	15×10^{-10}(b,e)	(3)
1.1×10^{-11}	(21)	0.61×10^{-10}	1.0×10^{-10}	4.3×10^{-10}(c,e)	(3)
1.6×10^{-11}	(22)	0.88×10^{-10}	1.5×10^{-10}	6.0×10^{-10}(d,e)	(3)
3.5×10^{-11}	(22)	1.9×10^{-10}	3.3×10^{-10}	1.7 to 27×10^{-10}(f)	(23)
6.8×10^{-11}	(22)	3.7×10^{-10}	6.4×10^{-10}	2.3×10^{-10}(g)	(24)
17×10^{-11}	(22)	9.4×10^{-10}	16×10^{-10}	2.5×10^{-10}(g)	(25)
				5.0×10^{-10}	(26)
				3×10^{-10}(c,g)	(27)
				5×10^{-10}(g,h)	(27)
				1.6×10^{-10}	(28)

(a) Results from tracer studies have been multiplied by 1.29 to correct for correlation.

(b) Nickel surface prepared by abrasive tumbling prior to oxidation.

(c) Surface annealed prior to oxidation.

(d) Surface ground prior to oxidation.

(e) Average value for the period 1 to 10 h.

(f) This range of values includes many of the early studies; the higher k_p values may well be a consequence of the less pure nickel used for early studies.

(g) A pressure dependence $k_p \propto p^{1/6}$ was used where experiments were performed at oxygen pressures other than 0.21 atm.

(h) Surface abraded prior to oxidation.

TABLE 4(a)

VALUES[a] AT 1100°C FOR THE EXPONENT m IN THE RATE EQUATION $(\Delta W/A)^m = k\ t$

Alloy	m for period 0.1 h < t < 1 h	m for period 1 h < t < 10 h	m for period 10 h < t < 164 h
Ni-270	1.86	1.96	1.80
Ni-270	1.89	1.94	
Ni-0.9Si	1.95	2.01	2.06
Ni-0.9Si	2.01	2.04	2.03
Ni-1.9Si	2.35	2.7	2.6 to 2.3
Ni-1.9Si	2.29	2.6	2.4 to 2.2
Ni-3.1Si	4.0 to 3.5	3.5 to 2.7	2.7 to 3.6
Ni-3.1Si	4.0	3.0	3.0
Ni-4.2Si	2.7	2.3	2.3 to 2.0
Ni-4.2Si	3.0 to 2.5	2.1	2.0 to 1.5
Ni-4.7Si	2.8 to 2.3	1.9	1.7 to 1.9
Ni-4.7Si	1.8	1.7	1.8 to 1.9
Ni.5.2Si	4	2.6 to 2.0	1.8
Ni-5.2Si	4	3.0 to 1.8	1.8
Ni-4.4Si-0.1Mg	7	2.4	2.0 to 3.6
Ni-4.4Si-0.1Mg	10 to 4	4.3 to 2.2	1.8 to 3.4

[a] Values derived from duplicate experiments

TABLE 4(b)

VALUES[a] OF THE EXPONENT m AT 1000, 1100 AND 1200°C

Alloy	Temperature °C	m for period 0.1 h < t < 1 h	m for period 1 h < t < 10 h	m for period 10 h < t 164 h
Ni-0.9Si	1000	2.24	1.88	1.9 to 2.4
Ni-0.9Si	1000	1.99	1.89	2.0 to 2.2
Ni-0.9Si	1100	1.95	2.01	2.06
Ni-0.9Si	1100	2.01	2.04	2.03
Ni-0.9Si	1200	2.03	2.20	2.2 to 1.9
Ni-0.9Si	1200	1.85	2.45	2.1 to 1.8
Ni-5.2Si	1000	3	2.4	2.4
Ni-5.2Si	1000	5	2.6 to 2.0	1.6
Ni-5.2Si	1100	4	2.6 to 2.0	1.8
Ni-5.2Si	1100	4	3.0 to 1.8	1.8
Ni-5.2Si	1200	2	2.3 to 3.7	3.0 to 2.4
Ni-5.2Si	1200	>4	3.0 to 2.4	2.2

[a]Values derived from duplicate experiments.

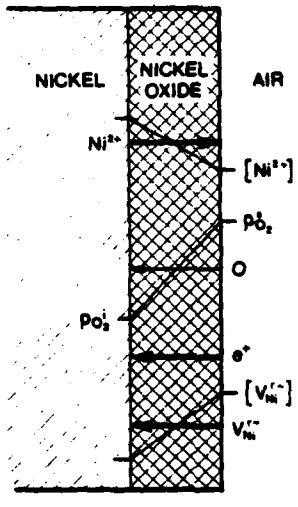

FIG. 1 Schematic representation of the transport of reactants for the high temperature oxidation of nickel. The dominant diffusion process contributing to oxide growth is outward diffusion of nickel ions, which can be described also in terms of an inward flow of nickel ion lattice vacancies $V_{Ni}^{''}$. Inward oxygen diffusion via oxide grain boundaries also contributes to oxide growth, and an electron hole current flows to balance the nickel ion charge transport.

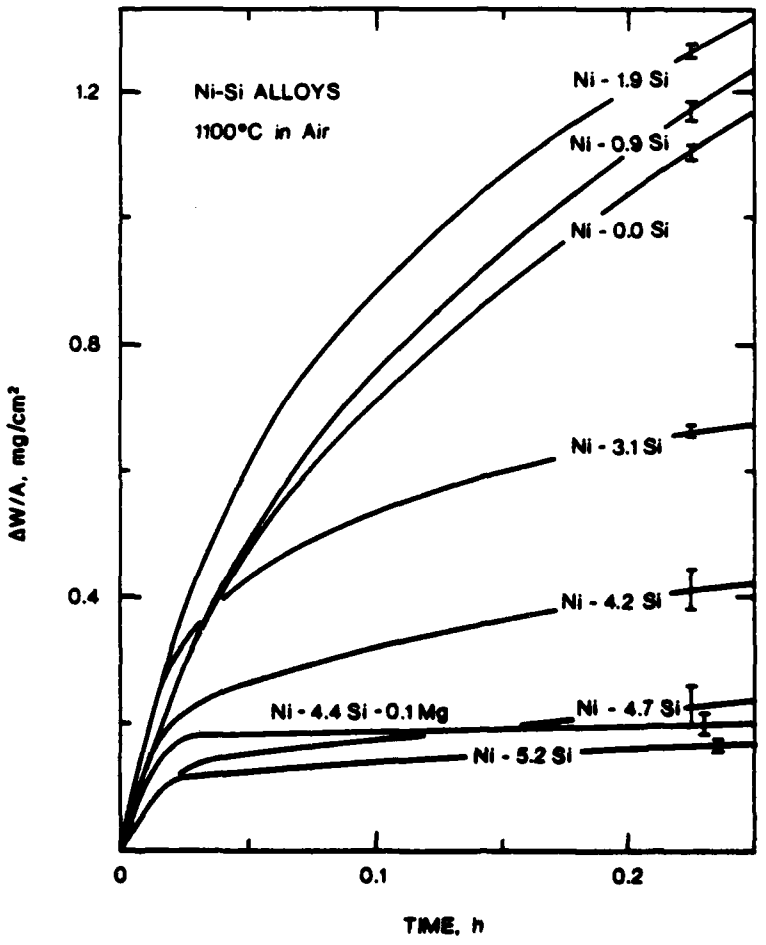

Fig. 2 Short-term specific weight gain curves for Ni-Si alloys oxidizing in air at 1100°C. The error bar represents the deviation of individual experimental curves from the averaged curve presented.

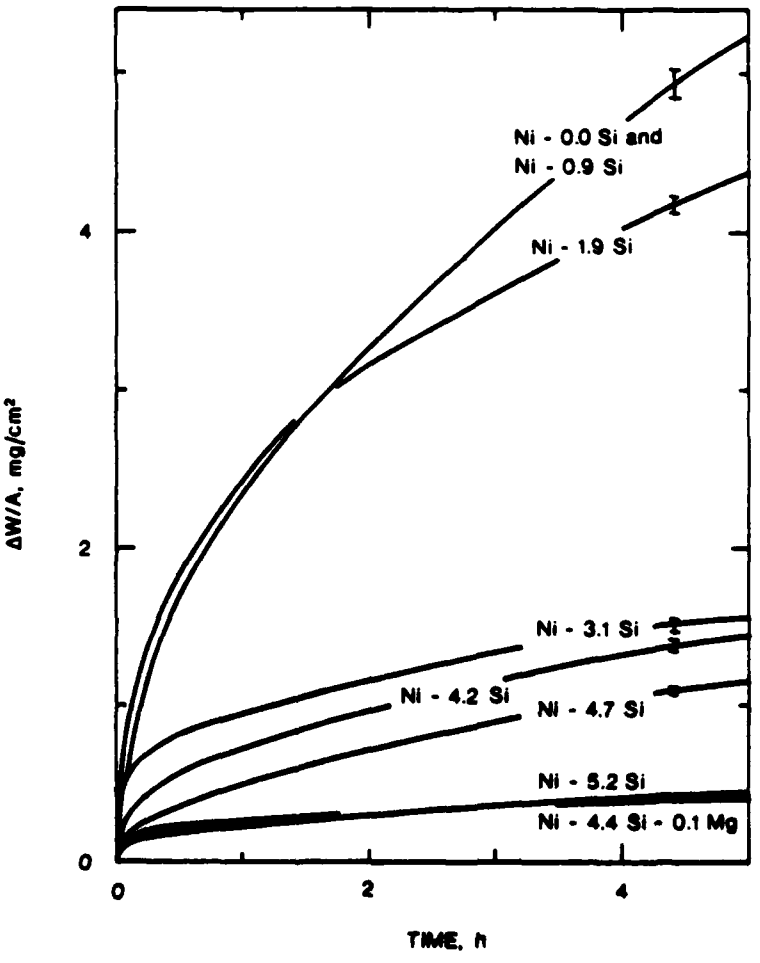

Fig. 3 Medium-term specific weight gain curves for Ni-Si alloys oxidising in air at 1100°C.

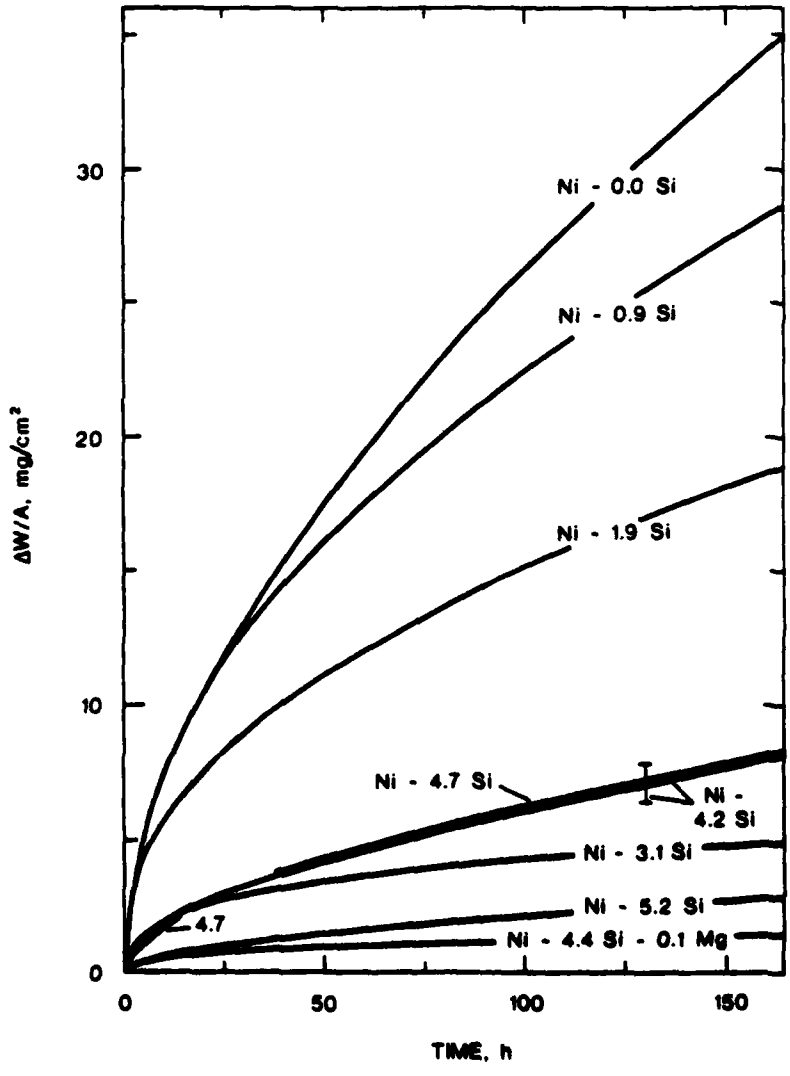

Fig. 4 Long-term specific weight gain curves for Ni-Si alloys oxidising in air at 1100°C. Apart from Ni-4.2Si, the alloys showed highly reproducible long-term curves.

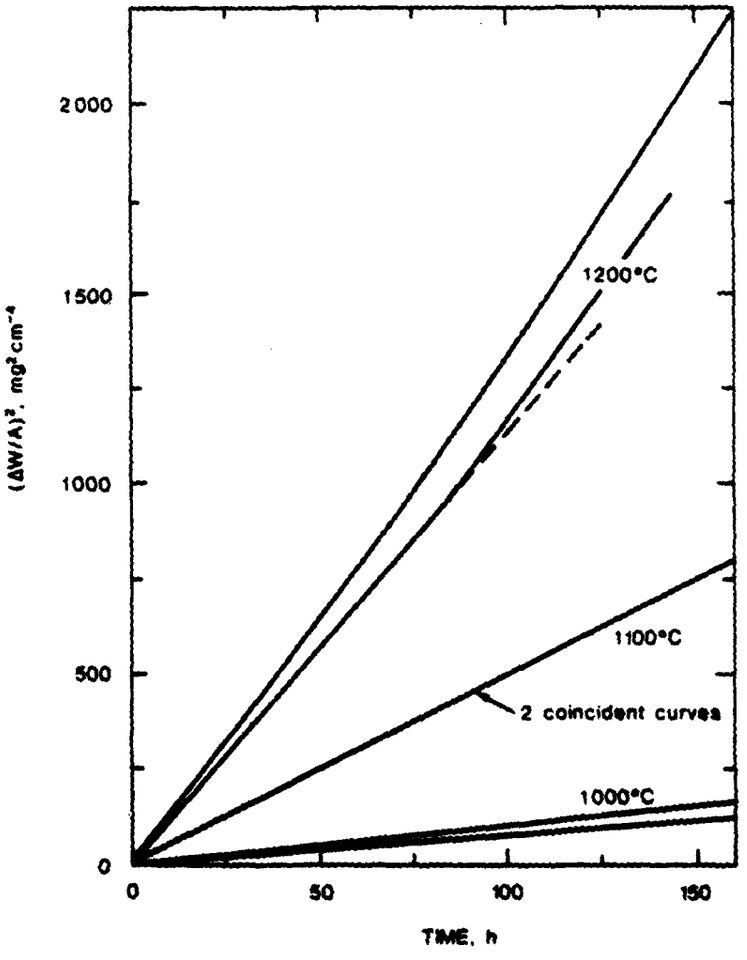

Fig. 5 Influence of temperature on the oxidation rate of Ni-0.9Si; duplicate results are shown for each temperature. The square of the specific weight gain has been used for these plots to allow easy assessment of conformity with a parabolic rate law. The dotted line for one of the 1200°C results represents long-term parabolic oxidation.

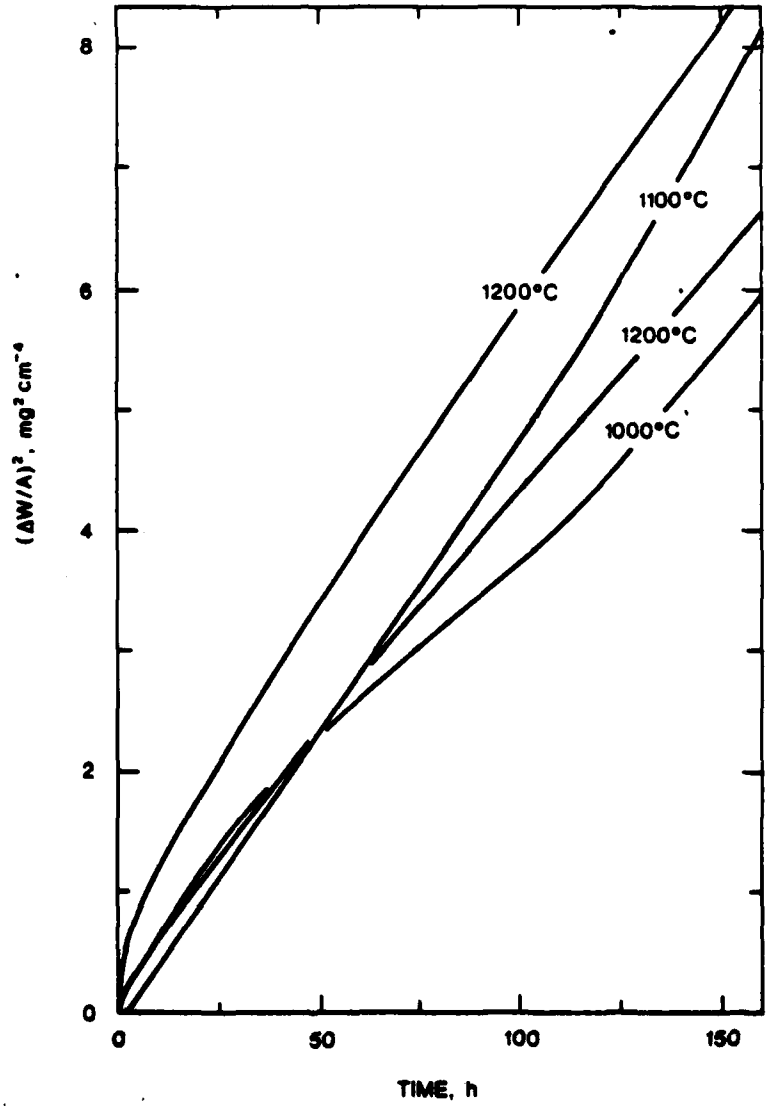

FIG. 6 Influence of temperature on the oxidation rate of Ni-5.2Si.

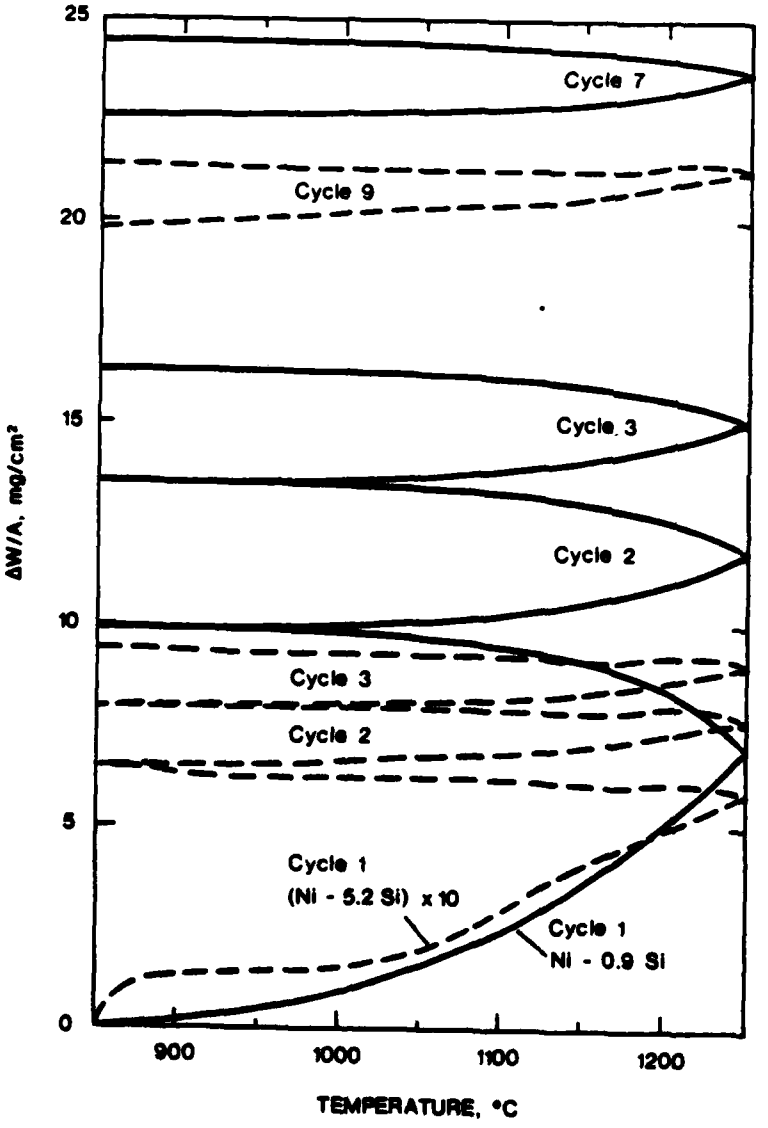

Fig. 7 Specific weight gain curves for Ni-0.9Si and Ni-5.2Si under conditions of cyclicly-varying temperature. Temperature was varied at a precisely controlled rate in the range 1.00 to 1.12°C min^{-1}. Data for Ni-5.2Si has been plotted with a multiplication factor of 10.

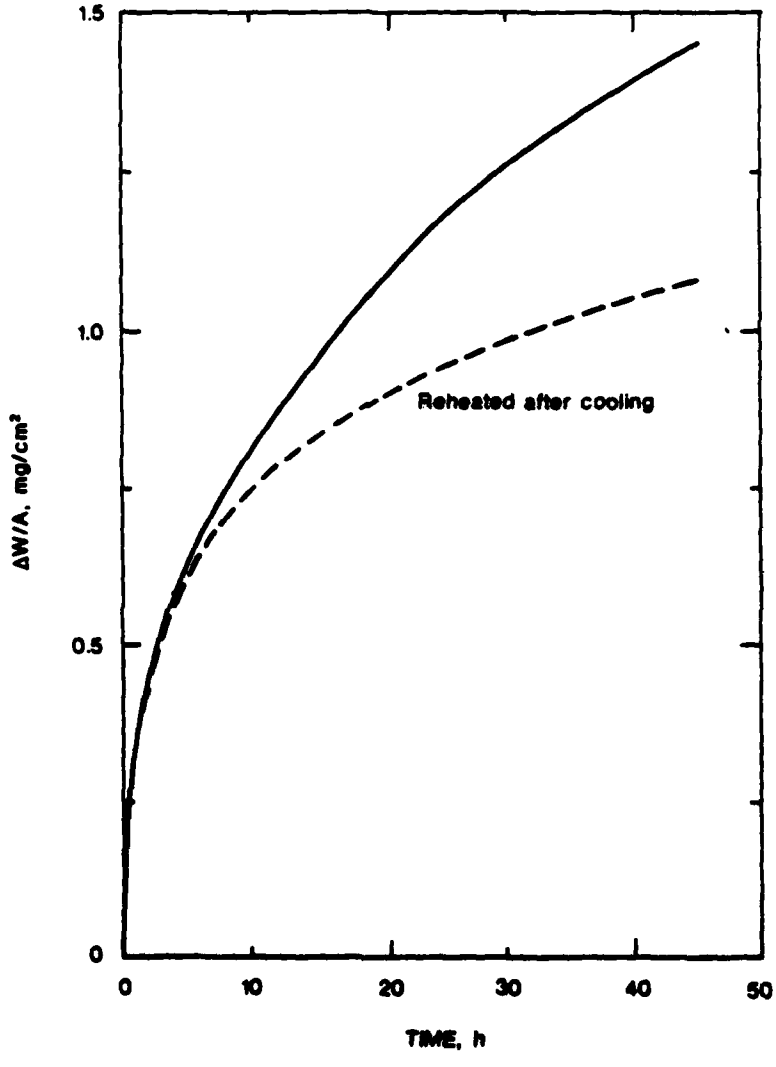

Fig. 8 Comparison of specific weight gain curves for Ni-5.2Si at 1000°C, showing the lower oxidation rate (lower curve) after the alloy has been heated for 164 h at 1000°C (upper curve) and then cooled at 20°C prior to reheating.

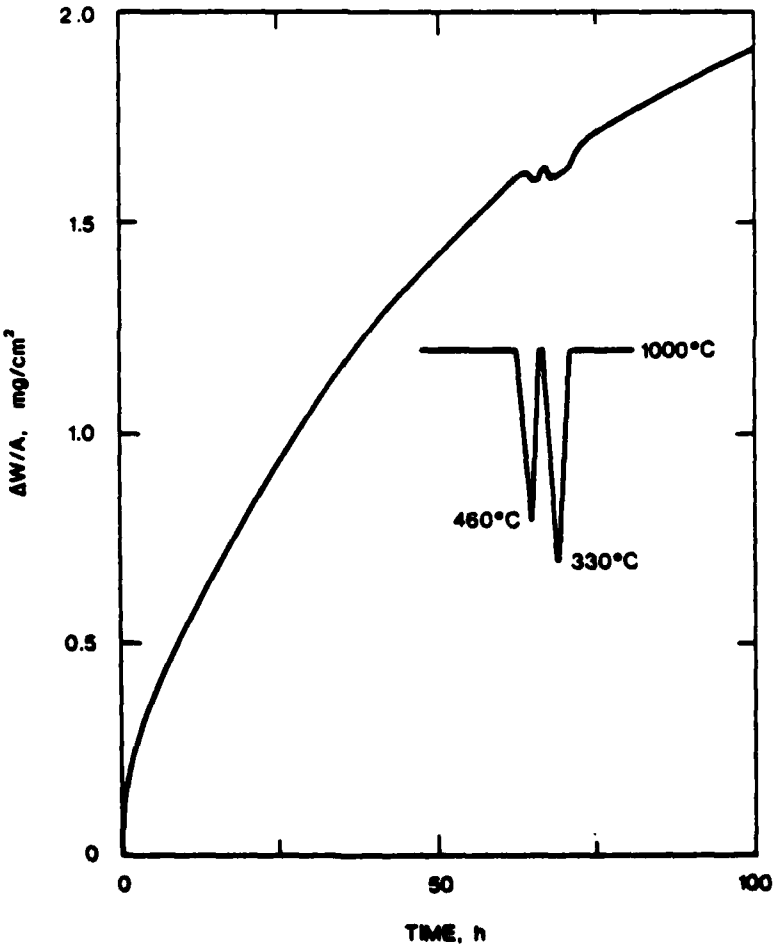

Fig. 9 Effect of temperature excursions to 460°C and 330°C during the oxidation of Ni-5.2Si at 1000°C. Only minor spallation of oxide occurred.

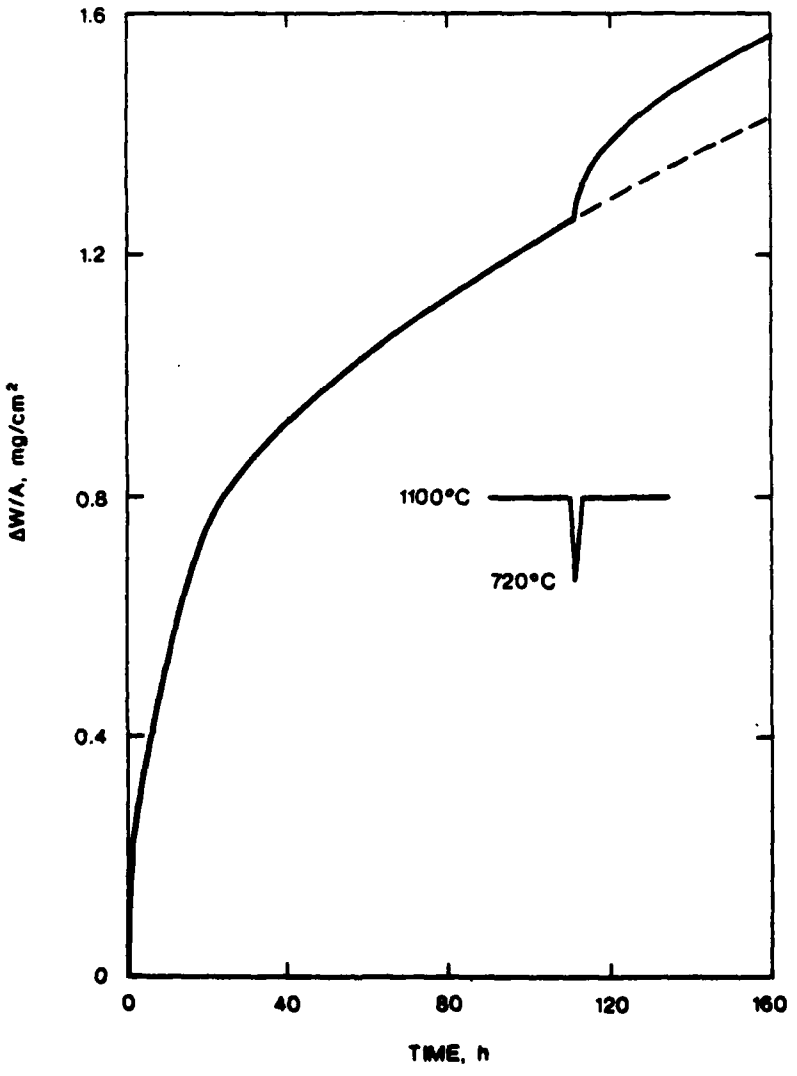

Fig. 10 Effect of a temperature excursion to 720°C during the oxidation of Nisil at 1100°C. The faster oxidation rate when the temperature of 1100°C was resumed indicates damage to the protective oxide scales even though no gross spallation occurred.

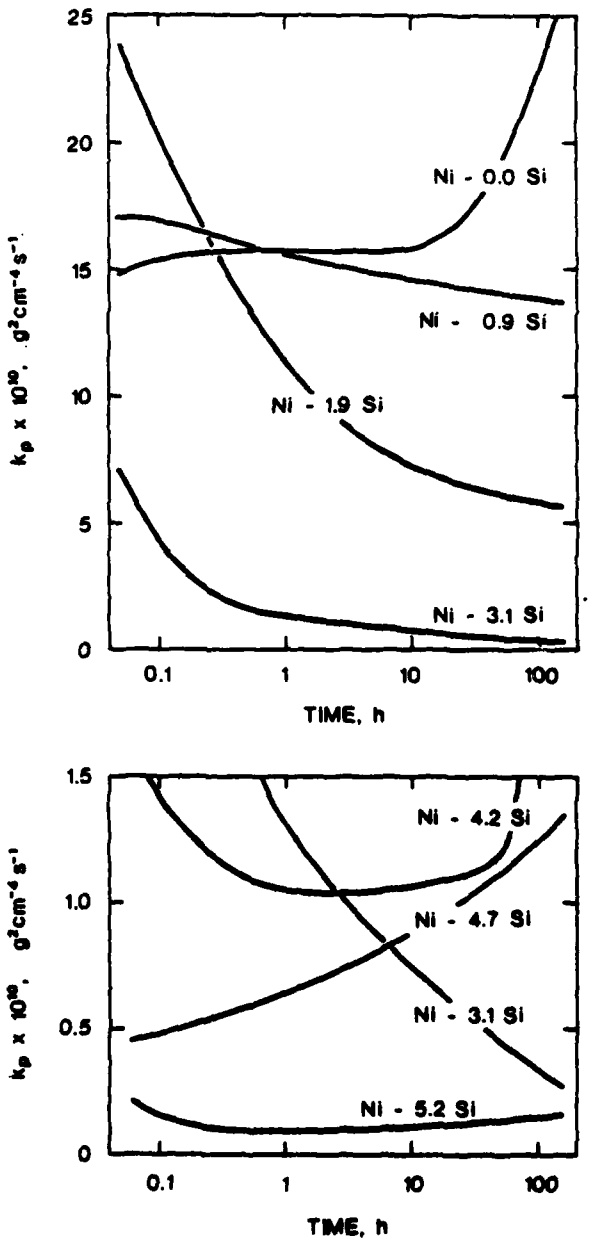

Fig. 11 (a) and (b). Parabolic rate constant, k_p, as function of time for Ni-Si alloys oxidising at 1100°C.

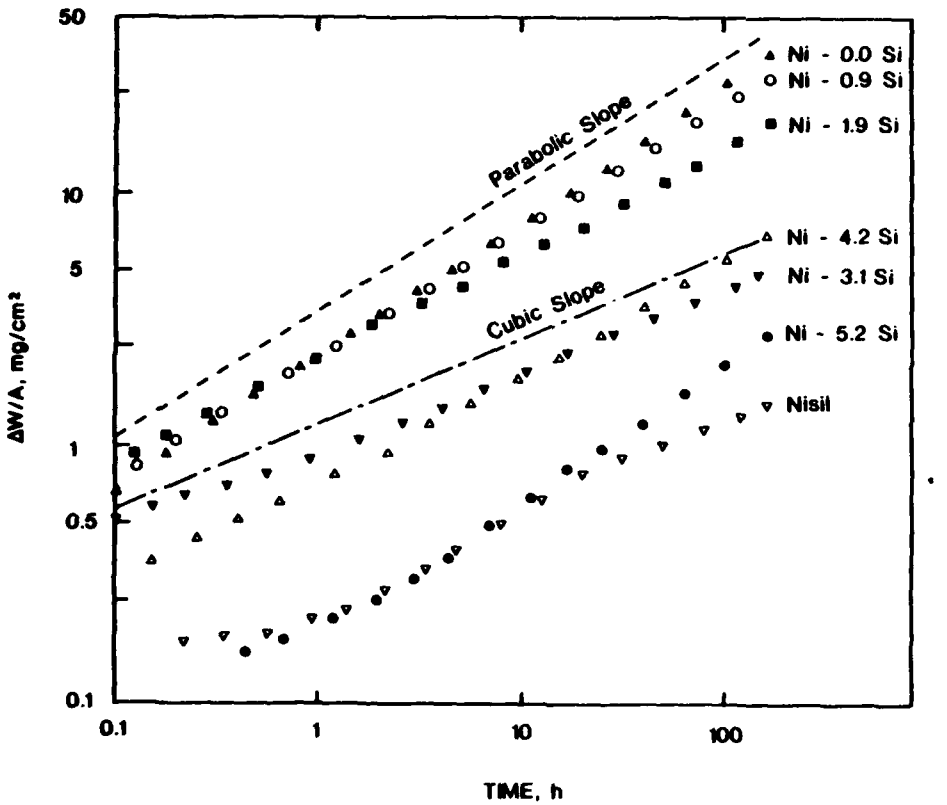

FIG. 12 Logarithmic plot of the thermogravimetric data from Figs. 2, 3 and 4, from which the values of n presented in Table 4(a) were derived.

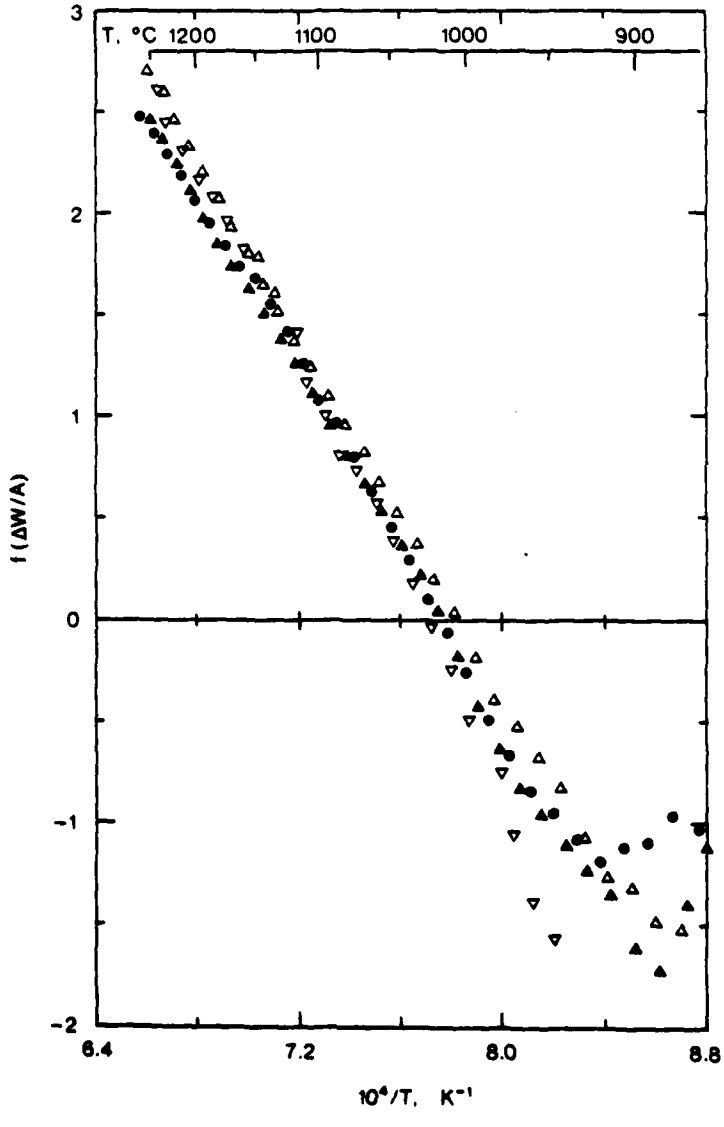

Fig. 13 Plot of the function $f(\Delta W/A) = \ln(\Delta W/A) + \ln d(\Delta W/A)dt$ against reciprocal temperature for Ni-0.9Si. ▽ - first cycle, increasing temperature; △ - first cycle decreasing temperature; ● - second cycle, increasing temperature; ▲ - second cycle, decreasing temperature.

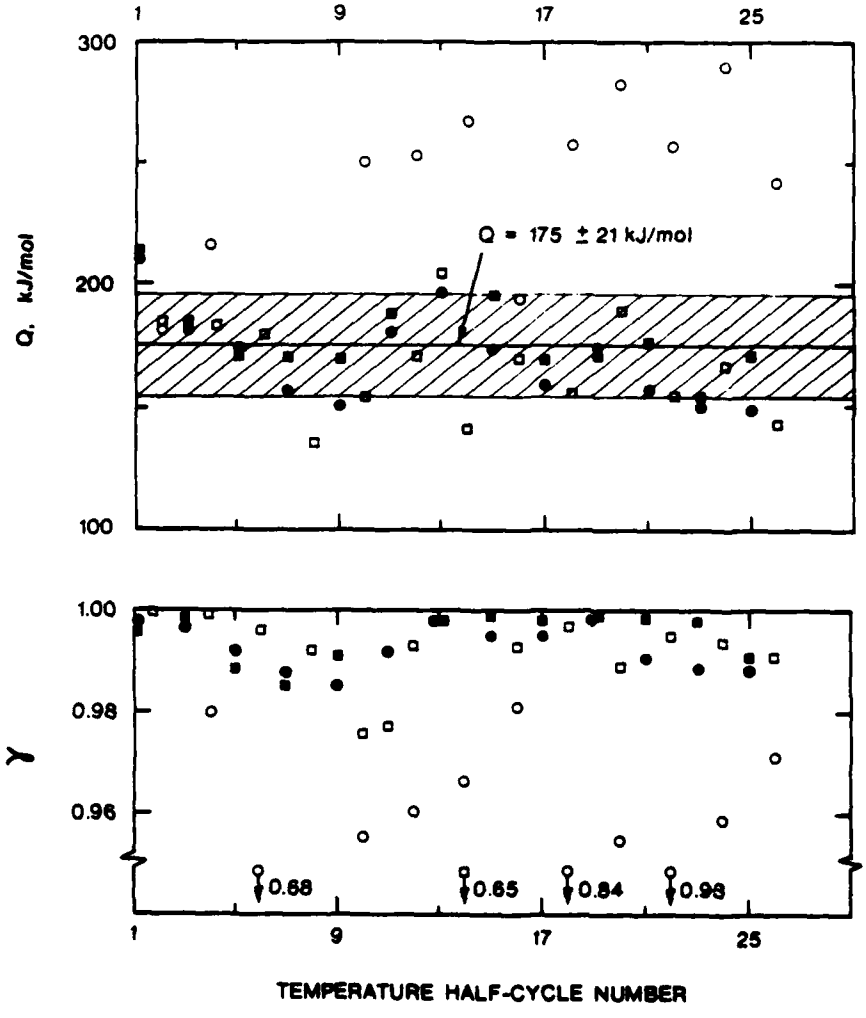

Fig. 14 Average activation energy Q for Ni-0.9Si for temperatures from 950 to 1250°C derived from plots such as Fig. 13. Data presented is from duplicate experiments, with values of Q derived during increasing temperature conditions represented by the symbols ● and ■, whereas the symbols ○ and □ denote decreasing temperature conditions. The lower graph shows the least-squares correlation coefficient γ applicable to the values of Q in the upper curve.

(MRL-R-887)

DISTRIBUTION LIST

MATERIALS RESEARCH LABORATORIES

Director
Superintendent, Metallurgy Division
Dr G.R. Johnston
Library (2 copies)

DEPARTMENT OF DEFENCE

Chief Defence Scientist (for CDS/DCDS/CPAS/CERPAS) (1 copy)
Army Scientific Adviser
Air Force Scientific Adviser
Navy Scientific Adviser
Officer-in-Charge, Document Exchange Centre (17 copies)
Technical Reports Centre, Defence Central Library
Central Office, Directorate of Quality Assurance - Air Force
Deputy Director Scientific and Technical Intelligence,
Joint Intelligence Organisation
Librarian, Bridges Library
Librarian, Engineering Development Establishment
Defence Science Representative, Australia High
Commission, London (Summary Sheets only)
Counsellor Defence Science, Washington, D.C. (Summary Sheets only)
Librarian, (Through Officer-in-Charge), Materials Testing
Laboratories, Alexandria, NSW
Senior Librarian, Aeronautical Research Laboratories
Senior Librarian, Defence Research Centre Salisbury, SA

DEPARTMENT OF DEFENCE SUPPORT

Deputy Secretary, DDS
Head of Staff, British Defence Research & Supply Staff (Aust.)

OTHER FEDERAL AND STATE DEPARTMENTS AND INSTRUMENTALITIES

NASA Canberra Office, Woden, ACT
The Chief Librarian, Central Library, CSIRO
Library, Australian Atomic Energy Commission Research Establishment

MISCELLANEOUS - AUSTRALIA

Librarian, State Library of NSW, Sydney NSW
University of Tasmania, Morris Miller Lib., Hobart, Tas.

DISTRIBUTION LIST
(continued)

MISCELLANEOUS

Library - Exchange Desk, National Bureau of Standards, USA.
UK/USA/CAN/NZ ABCA Armies Standardisation Representative (4 copies)
Director, Defence Research Centre, Kuala Lumpur, Malaysia
Exchange Section, British Library, UK
Periodicals Recording Section, Science Reference Library,
British Library, UK
Library, Chemical Abstracts Service
INSPEC: Acquisition Section, Institute of Electrical Engineers, UK
Engineering Societies Library, USA
Aeromedical Library, Brooks Air Force Base, Texas, USA
Ann Germany Documents Librarian, The Centre for Research
Libraries, Chicago Ill.
Defense Attache, Australian Embassy, Bangkok, Thailand
(Att. D. Pender)

ADDITIONAL DISTRIBUTION

Dr Lawrence D. Palmer, Ampol Research & Development Laboratory,
Brisbane, Queensland

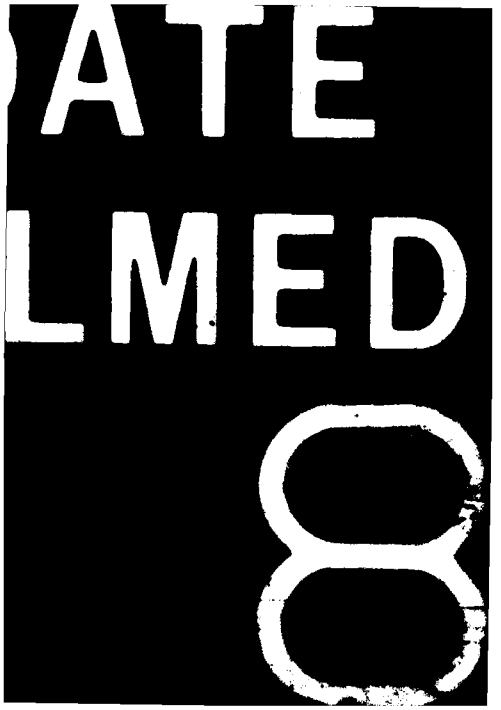
ATE
LMED
8